Analytical derivation of the Budyko curve based on rainfall characteristics and a simple evaporation model

A. M. J. Gerrits,[1,2] H. H. G. Savenije,[1] E. J. M. Veling,[1] and L. Pfister[2]

Received 24 July 2008; revised 18 November 2008; accepted 23 January 2009; published 3 April 2009.

[1] The Budyko curve is often used to estimate the actual evaporation as a function of the aridity index in a catchment. Different empirical equations exist to describe this relationship; however, these equations have very limited physical background. The model concept presented in this paper is physically based and uses only measurable parameters. It makes use of two types of evaporation: interception and transpiration. It assumes that interception can be modeled as a threshold process on a daily time scale. If multiplied with the rainfall distribution function, integrated, and multiplied with the expected number of rain days per month, the monthly interception is obtained. In a similar way, the monthly interception can be upscaled to annual interception. Analogous to the interception process, transpiration can be modeled as a threshold process at a monthly time scale and can be upscaled by integration and multiplication with the expected number of rain months. The expected rain days per month are modeled in two ways: as a fixed proportion of the monthly rainfall and as a power function based on Markov properties of rainfall. The latter is solved numerically. It appears that on an annual basis the analytical model does not differ much from the numerical solution. Hence, the analytical model is used and applied on 10 locations in different climates. This paper shows that the empirical Budyko curve can be constructed on the basis of measurable parameters representing evaporation threshold values and the expected number of rain days and rain months and, in addition, a monthly moisture carryover amount for semiarid zones.

Citation: Gerrits, A. M. J., H. H. G. Savenije, E. J. M. Veling, and L. Pfister (2009), Analytical derivation of the Budyko curve based on rainfall characteristics and a simple evaporation model, *Water Resour. Res.*, *45*, W04403, doi:10.1029/2008WR007308.

1. Introduction

[2] In water resources modeling the Budyko curve is often used to simulate evaporation as a function of an aridity index in a simple supply-demand framework. In some locations of the world, annual evaporation may approach annual precipitation. This occurs if there is always sufficient energy available to evaporate the precipitation. Such locations are moisture constrained. In other locations, annual evaporation may approach potential evaporation. This happens if the available energy is less than the required energy to evaporate the annual precipitation. These locations are energy constrained. Depending on the dryness of the climate, either the available water or the available energy is the limiting factor.

[3] The Budyko curve is based on two balance equations: the water balance and the energy balance [*Arora*, 2002]:

$$\frac{\mathrm{d}S}{\mathrm{d}t} = P - E - Q \tag{1}$$

$$R_n = \rho\lambda E + H + G \tag{2}$$

where S is the water storage, P the precipitation, E actual evaporation, Q the catchment runoff, R_n the net radiation, λ the latent heat of vaporization, H the sensible heat flux, and G the ground heat flux. On an annual time scale we can assume that the water storage change is negligible ($\mathrm{d}S/\mathrm{d}t = 0$) and that the net ground heat flux approaches zero ($G = 0$). By dividing equation (2) by equation (1) we obtain with $P_a = E_a + Q_a$ where the subscript a indicates annual values:

$$\frac{R_n}{P_a} = \frac{\rho\lambda E_a}{P_a} + \frac{H}{P_a} \tag{3}$$

If we successively define the annual potential evaporation as $\rho\lambda E_p = R_n$ (where *Arora* [2002] interprets potential evaporation as all energy being converted into evaporation and none in heating) and define the Bowen ratio as $B_r = H/\rho\lambda E_a$ we obtain

$$\frac{E_p}{P_a} = \frac{E_a}{P_a} + \frac{B_r E_a}{P_a} = \phi = \frac{E_a}{P_a}(1 + B_r) \tag{4}$$

with ϕ the aridity index.

[4] Since the Bowen ratio can also be expressed as a function of the aridity index [*Arora*, 2002], equation (4) can be rewritten as

$$\frac{E_a}{P_a} = \frac{\phi}{1 + f(\phi)} = F(\phi) \tag{5}$$

[1]Water Resources Section, Delft University of Technology, Delft, Netherlands.
[2]Department of Environment and Agro-biotechnologies, Centre de Recherche Public-Gabriel Lippmann, Belvaux, Luxembourg.

0043-1397/09/2008WR007308$09.00

Table 1. Different Budyko Curves as a Function of the Aridity Index ϕ

Equation	Reference
$\frac{E_a}{P_a} = 1 - \exp^{-\phi}$	*Schreiber* [1904]
$\frac{E_a}{P_a} = \phi \tanh(1/\phi)$	*Ol'dekop* [1911]
$\frac{E_a}{P_a} = \frac{1}{\sqrt{0.9+(1/\phi)^2}}$	*Turc* [1954]
$\frac{E_a}{P_a} = \frac{1}{\sqrt{1+(1/\phi)^2}}$	*Pike* [1964]
$\frac{E_a}{P_a} = [\phi \tanh(1/\phi)(1 - \exp^{-\phi})]^{0.5}$	*Budyko* [1974]
$\frac{E_a}{P_a} = 1 - \frac{\phi \cdot \gamma^{\frac{\gamma}{\phi}-1} \exp^{-\gamma}}{\Gamma\left(\frac{\gamma}{\phi}\right) - \Gamma\left(\frac{\gamma}{\phi},\gamma\right)}$	*Porporato et al.* [2004]

[5] A lot of studies have been done on finding this relation. Classical studies were done by *Schreiber* [1904], *Ol'dekop* [1911], *Budyko* [1974], *Turc* [1954], and *Pike* [1964]. Their equations are summarized in Table 1 and plotted in Figure 1, with on the x axis the aridity index, which expresses the ratio of annual potential evaporation by annual precipitation (E_p/P_a). *Turc*'s [1954] curve is not shown in Figure 1, because it is similar to *Pike*'s [1964] curve. The observations are from several water balance models with different catchment sizes [*Perrin et al.*, 2007; *Samuel et al.*, 2008; C. Jothityangkoon and and M. Sivapalan, Framework for exploration of climatic and landscape controls on catchment water balance, with emphasis on inter-annual variability, submitted to *Journal of Hydrology*, 2008; H. H. G. Savenije, Lecture notes on hydrology of catchments, rivers and deltas, Delft University of Technology, 2003].

[6] Building on these almost fully empirical relationships, other authors attempted to incorporate more physics in the equations. For example, *Choudhury* [1999] added net radiation and a calibration factor α, *Zhang et al.* [2001, 2004] found a model parameter, w, describing the integrated effects of catchment characteristics like vegetation cover, soil properties and catchment topography. *Yang et al.* [2006, 2008] added a catchment parameter, *Donohue et al.* [2007] tried to include vegetation dynamics, and *Milly* [1993], *Porporato et al.* [2004], and *Rodríguez-Iturbe and Porporato* [2004] developed a stochastic model, that incorporated the maximum storage capacity. However, these relationships were still not fully physically based. Even the equation of *Yang et al.* [2008], who found an analytical derivation for the Budyko curve where they included a parameter n, representing catchment characteristics, contains a calibration factor. This extra parameter is a collection

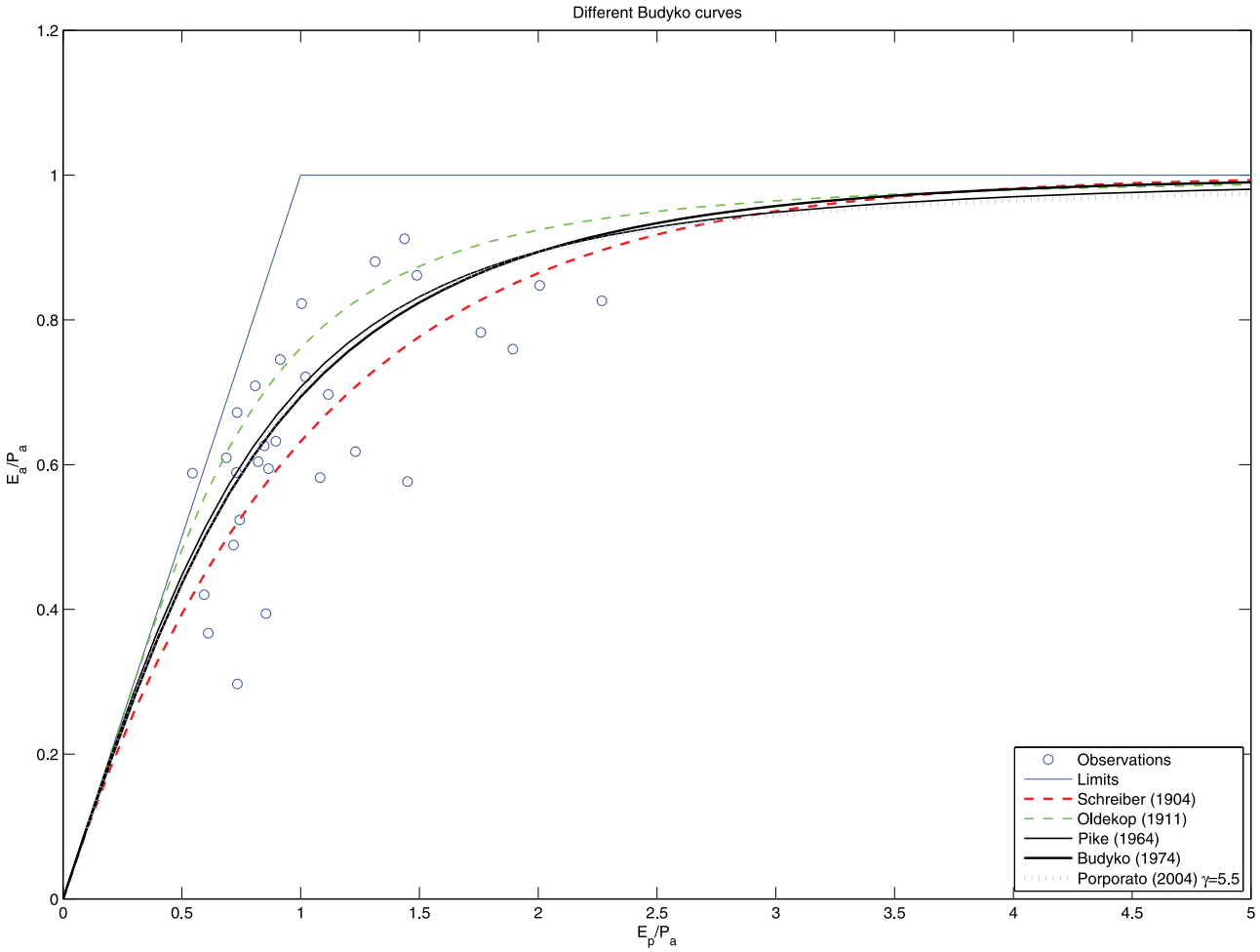

Figure 1. Different representations of the Budyko curves and some observations. The 1:1 limit expresses the limitation by available energy ($E_p < P_a$), and the horizontal limit expresses the limitation by available water ($E_p > P_a$).

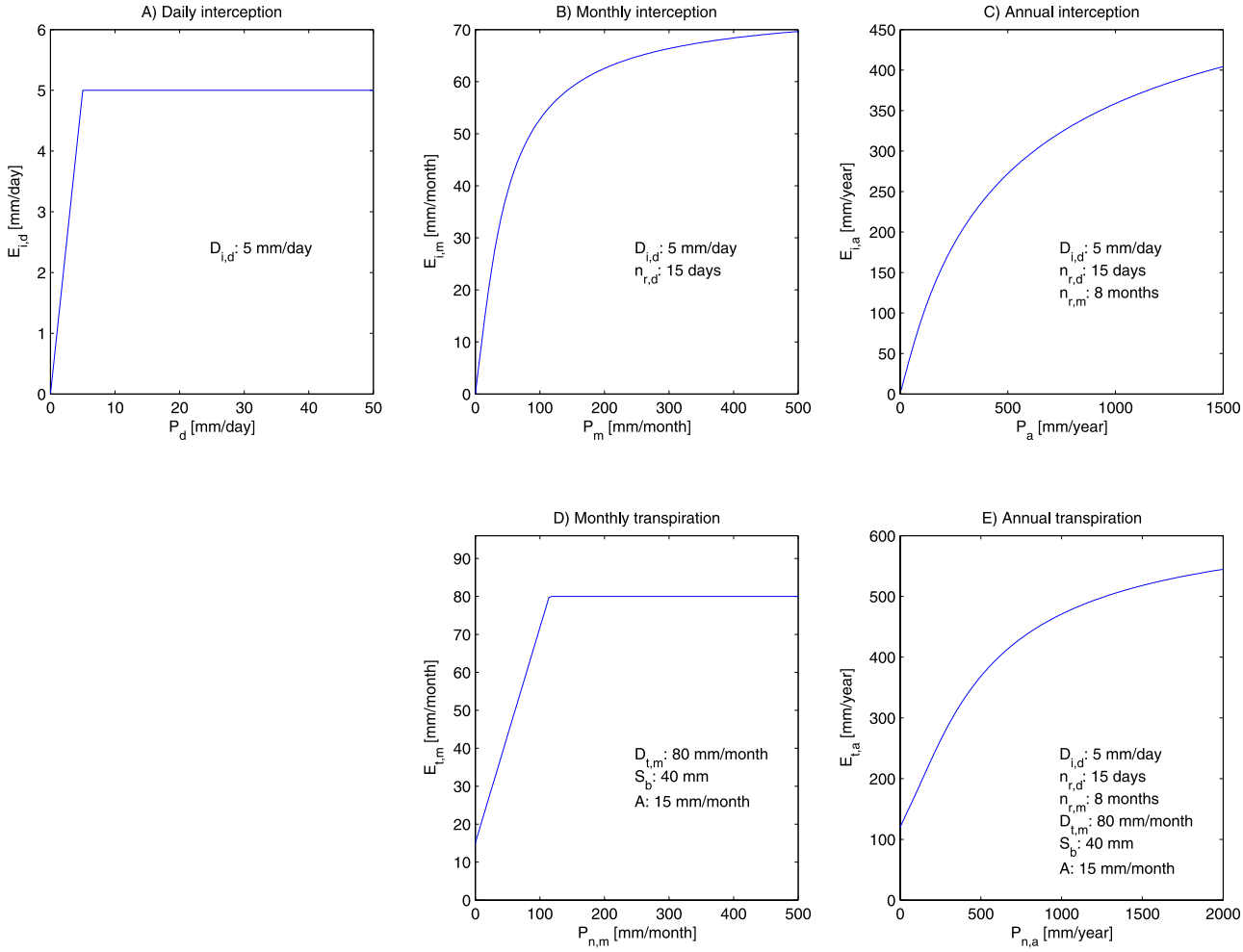

Figure 2. Stepwise integration from daily interception to annual interception and from monthly transpiration to annual transpiration.

of all kinds of catchment characteristics and is therefore difficult to determine or to measure. The aim of this paper is to find an analytical derivation of the Budyko curve based on a conceptual model and with only measurable parameters.

[7] The derivation considers evaporation as the mechanism that feeds water back to the atmosphere and that includes all evaporative processes as defined by, e.g., *Shuttleworth* [1993]:

$$E = E_i + E_t + E_o + E_s \tag{6}$$

Hence, evaporation includes evaporation from interception (E_i), transpiration (E_t), from open water (E_o), and from the soil (E_s). Interception is the evaporation from the entire wet surface, so not only the canopy, but also the understorey, the forest floor, and the top layer of the soil. Although the latter seems to have an overlap with soil evaporation, we distinguish them by the fact that soil evaporation refers to rainwater that is stored in the soil and is connected with the root zone [*de Groen and Savenije*, 2006]. In this paper we assume that evaporation from the deeper soil is not significant or can be combined with evaporation from interception. Open water evaporation is mainly important in areas where for example great lakes exist and is therefore not considered in this paper. Hence, the following equation is used to calculate total evaporation:

$$E = E_i + E_t \tag{7}$$

[8] An important distinction between the different types of evaporation is the time scale of the underlying processes. For example, interception is a process that has a short time scale in the order of 1 day or a few days. Generally, canopy interception has a very short time scale (less than 1 day), which can be observed by the fact that after a rainfall event the canopy is dry within a couple of hours. Forest floor interception, on the other hand, has a somewhat larger time scale, since it may take more time (one to several days) to dry the forest floor [*Gerrits et al.*, 2007; *Baird and Wilby*, 1999]. The time scale is estimated by dividing the stock by the flux. In the case of interception the stock amounts to a few millimeters and the evaporative flux is a few millimeters per day, resulting in the conclusion that interception has a time scale in the order of 1 day. Transpiration on the other hand has a much longer time scale [e.g., *Dolman and Gregory*, 1992; *Savenije*, 2004; *Scott et al.*, 1995]. For transpiration the stock is in the order of tens to hundreds of millimeters, while the flux is a few millimeters per day

Table 2. Characteristics of Investigated Locations in This Paper

Place	Location	Altitude (m)	P_a [a] (mm/a)	E_p [b] (mm/a)	Data Availability P [c]
Harare (Zimbabwe)	17.9°S, 31.1°E	1500	793.8	1319	1950–1995 (44)
Masvingo (Zimbabwe)	20.0°S, 30.9°E	1100	624.9	1344	1951–1996 (44)
Bulawayo (Zimbabwe)	20.2°S, 28.6°E	1340	597.0	1378	1950–1996 (45)
Peters Gate (South-Africa)	34.0°S, 18.6°E	37	524.9	1051	1951–2006 (50)
Hyderabad (India)	17.5°N, 78.5°E	545	785.6	1512	1871–2006 (121)
Indianapolis (Indiana, USA)	39.7°N, 86.3°W	241	1024.5	816	1861–2007 (141)
Kansas City (Missouri, USA)	39.3°N, 94.7°W	297	928.6	841	1871–2003 (121)
Sheridan (Wyoming, USA)	44.8°N, 106.8°W	1144	381.3	642	1894–2004 (98)
Tallahassee (Florida, USA)	30.4°N, 84.4°W	17	1503.7	1139	1886–2005 (114)
Lyamungu (Tanzania)	3.2°S, 37.3°E	1337	1586.9	1567	1936–2003 (67)

[a]Global Historical Climatology Network (GHCN) version 2 database.
[b]AHN, Remote Sensing and Image Research Center.
[c]Number of years is given in parentheses.

Gerrits et al. [2009] and *Baird and Wilby* [1999], resulting in a time scale in the order of month(s).

2. Methodology

[9] When creating a model, it is important to model the different processes at the right time scale. If one wants to make a monthly interception model, it is imperative to use daily information on the precipitation. For the total amount of interception, it is important to know the rainfall intensity and the time between rainfall events. It makes a large difference if monthly rainfall consists of many small events, or a few very large events. A monthly interception model does not necessarily require the actual daily rainfall data, but it does need information on the daily rainfall distribution (e.g., Markov properties). This is the main idea behind the proposed model: we model the evaporation process at the time scale on which it occurs and upscale it by making use of the temporal characteristics of the rainfall.

[10] In Figure 2 an overview of the model is shown. At a daily time scale interception can be modeled as a simple threshold process: all rainwater is intercepted as long as the storage capacity is not exceeded. Hereafter water will infiltrate or run off (see experiments of, e.g., *Deguchi et al.* [2006], *Helvey and Patric* [1965], *Rutter et al.* [1971], and *Viville et al.* [1993]). When we have information on how the rainfall is distributed over the month it is possible to upscale daily interception to monthly interception. Analogously, we can upscale monthly interception to annual interception, if we have information on how monthly rainfall is distributed over the year.

[11] Similar to interception, we can model transpiration as a threshold process at a monthly time scale as a function of net precipitation (rainfall minus interception). If the temporal characteristics of the net rainfall are known, we can upscale monthly transpiration to annual transpiration. Finally, summing annual interception and transpiration gives an expression for annual evaporation as a function of annual precipitation.

[12] In the following sections, the model will be described in more detail. In section 3 an analytical derivation of the model is presented. For the analytical solution we had to simplify the Markov properties of the daily rainfall. In section 4 we derive a model that takes full account of the Markov properties. Both the analytical and numerical derivations are carried out with the mathematical software package MAPLE 9.5 (Waterloo Maple Inc.).

[13] For this study ten locations in different parts of the world have been investigated. In Table 2 the characteristics of the locations are given. These ten locations have been chosen because both climate data and Markov coefficients were available. In the last column the available time series are shown together with the number of years used in the analysis. Only those years have been used that had complete monthly rainfall series.

[14] The monthly rainfall data have been obtained from the Global Historical Climatology Network (GHCN) database, downloadable from http://climexp.knmi.nl. The annual potential evaporation data has been retrieved from the AHN, Remote Sensing and Image Research Center (Chiba University), downloadable from http://www-cger.nies.go.jp/grid-e/. The potential evaporation has been calculated with the Priestley-Taylor method [*Priestley and Taylor*, 1972].

3. Analytical Derivation Without Markov Properties

3.1. Monthly Interception Equation (Analytical)

[15] On a daily basis, interception is a typical threshold process [e.g., *Savenije*, 1997, 2004]. Rainwater is intercepted by the canopy, the forest floor, or any other body as long as the storage capacity is not exceeded. When the storage capacity is reached maximum interception is achieved. Hence daily evaporation from interception ($E_{i,d}$) can be modeled as

$$E_{i,d} = \min\left(D_{i,d}, P_d\right) \tag{8}$$

here $D_{i,d}$ is the daily interception threshold [L T^{-1}], and P_d the daily rainfall on a rain day [L T^{-1}] (see Figure 2a).

[16] Since we want to model interception on a monthly time scale, we have to make use of daily rainfall characteristics. As shown by many authors [*Sivapalan and Blöschl*, 1998; *Todorovic and Woolhiser*, 1975; *Woolhiser et al.*, 1993; *de Groen and Savenije*, 2006], the probability distribution of rainfall on a rain day can be described as

$$f_{i,d}(P_d) = \frac{1}{\beta}\exp\left(\frac{-P_d}{\beta}\right) \tag{9}$$

β [L T^{-1}] being the scaling factor, equal to the expected rainfall on a rain day, which can be expressed as

$$\beta = P_m / \mathrm{E}\left(n_{r,d} | n_m\right) \tag{10}$$

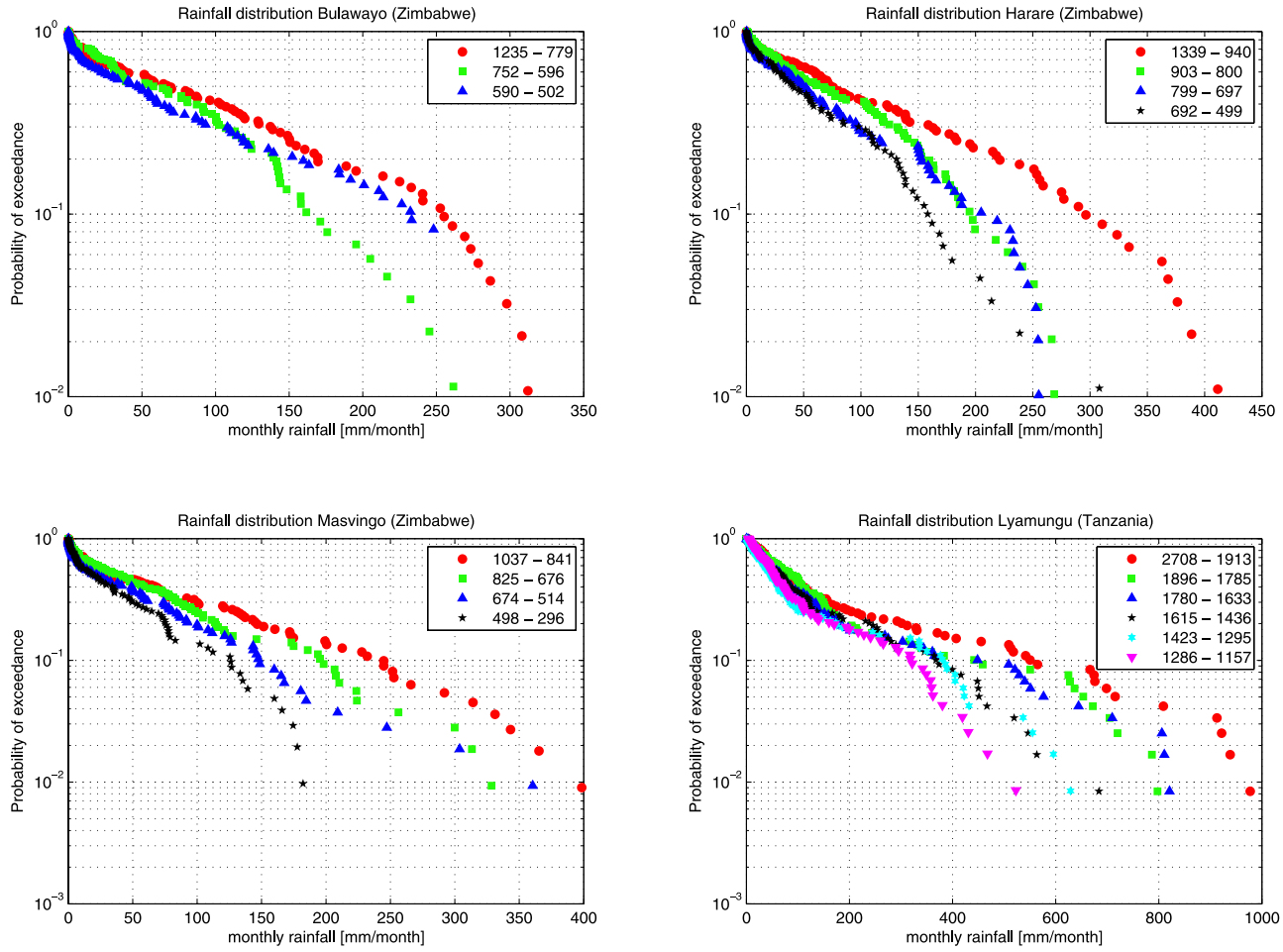

Figure 3. Probability of exceedance of rainfall amounts on rain months for different stations in Zimbabwe and Tanzania. The slope equals $-1/\kappa_m$.

with P_m [L T^{-1}] being the monthly rainfall and $n_{r,d}$ and n_m the number of rain days per month and amount of days per month, respectively.

[17] Multiplying equations (8) and (9) [*de Groen*, 2002] and integrating with respect to P_d from zero to $D_{i,d}$ (events which are too small to fill the storage capacity) and subsequently from $D_{i,d}$ to infinity (events which are larger than the storage capacity) leads to the average interception per day. Successively, multiplying the average interception per day with the expected rain days per month leads to equation (11), which is plotted in Figure 2b:

$$E_{i,m} = \mathrm{E}(n_{r,d}|n_m)\int_0^{\infty} E_{i,d}\cdot f_{i,d}(P_d)\mathrm{d}P_d = P_m\left(1-\exp\left(\frac{-D_{i,d}}{\beta}\right)\right) \quad (11)$$

If combined with equation (10), $D_{i,d}/\beta$ is equal to the potential amount of monthly interception divided by the monthly rainfall, which is a sort of aridity index, $\phi_{i,m}$ [−]. Equation (11) can then be rewritten as

$$E_{i,m} = P_m\left(1-\exp\left(-\phi_{i,m}\right)\right) \quad (12)$$

3.2. Annual Interception Equation (Analytical)

[18] To upscale monthly interception to annual interception, we make use of the probability distribution of rainfall in a rain month, which can also be described by an exponential function:

$$f_{i,m}(P_m) = \frac{1}{\kappa_m}\exp\left(\frac{-P_m}{\kappa_m}\right) \quad (13)$$

with κ_m [L T^{-1}] as the monthly scaling factor.

[19] This relation is confirmed by the straight lines obtained when monthly rainfall is plotted against the logarithm of the probability of exceedance for all locations in Table 2. As an illustration the results for Zimbabwe and Tanzania are shown in Figure 3. Although at high rainfall amounts the line tends to deviate from the straight line, we may neglect this, because our interest is not on extreme rainfall amounts. In addition, the uncertainty of the extreme rainfall is large since they are based on a small number of events. However, we realize that in some climates these extreme events may be significant for the annual water balance.

[20] Analogous to β, κ_m equals to the expected rainfall in a rain month expressed as

$$\kappa_m = P_a/\mathrm{E}(n_{r,m}|n_a) \quad (14)$$

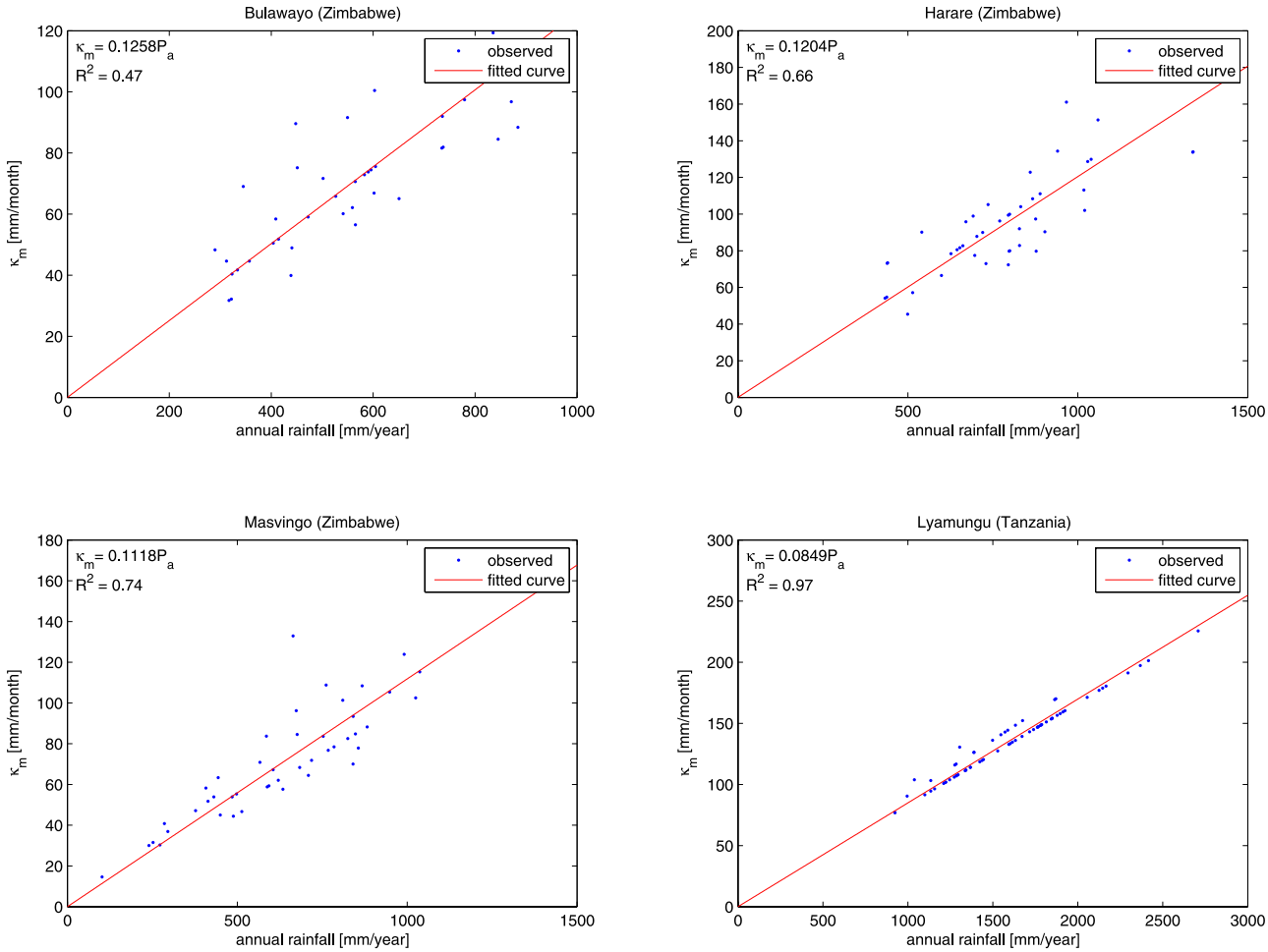

Figure 4. Scaling factor κ_m can be assumed to be directly proportional to the annual rainfall.

where P_a [L T^{-1}] is the annual rainfall, $n_{r,m}$ the number of rain months in a year, and n_a the number of months per year. Since the number of rain months per year is constant for a given location, the scaling factor κ_m is directly proportional to P_a. This is confirmed by the high regression values in Figure 4 and Table 3 (only the results of Tanzania and Zimbabwe are shown). A rain month is defined as a month with more than 2 mm/month of rain.

Table 3. Expected Number of Rain Days for the Analytical Solution and for the Numerical Solution With Power Functions Coefficients Describing Markov Probabilities[a]

		Numerical						
	Analytical	$p_{01} = q(P_m)^r$		$p_{11} = u(P_m)^v$		Analytical/Numerical		
Location	$n_{r,d}$[b]	q	r	u	v	$n_{r,m}$[c]	$n_{nr,m}$[c]	A[d] (mm/month)
Harare	15	0.020	0.55	0.200	0.24	8.3 (0.66)	7.4 (0.74)	15
Masvingo	11	0.030	0.43	0.200	0.24	8.9 (0.74)	6.9 (0.67)	15
Bulawayo	10	0.044	0.34	0.200	0.24	7.9 (0.47)	6.6 (0.60)	15
Peters Gate	11	0.094	0.33	0.034	0.40	11.2 (0.85)	8.1 (0.74)	5
Hyderabad	10	0.092	0.38	0.024	0.53	8.6 (0.72)	6.7 (0.68)	20
Indianapolis	11	0.129	0.30	0.045	0.42	12.0 (1.00)	11.7 (0.96)	0
Kansas City	11	0.129	0.27	0.061	0.30	11.8 (0.97)	10.6 (0.85)	0
Sheridan	10	0.216	0.22	0.084	0.30	11.7 (0.95)	6.2 (0.72)	0
Tallahassee	15	0.127	0.29	0.017	0.55	11.8 (0.99)	11.5 (0.95)	0
Lyamungu	17	0.053	0.39	0.170	0.20	11.8 (0.97)	10.1 (0.77)	0

[a]The analytical solution is from equations (16) and (23). Also given are the number of rain months per year (for gross, $n_{r,m}$, and net, $n_{nr,m}$, rainfall) and the carryover value A for different locations. Markov probabilities are taken from *de Groen and Savenije* [2006].
[b]CRU TS 2.1. Only wettest months are used.
[c]Value in parentheses is r^2.
[d]Estimated values.

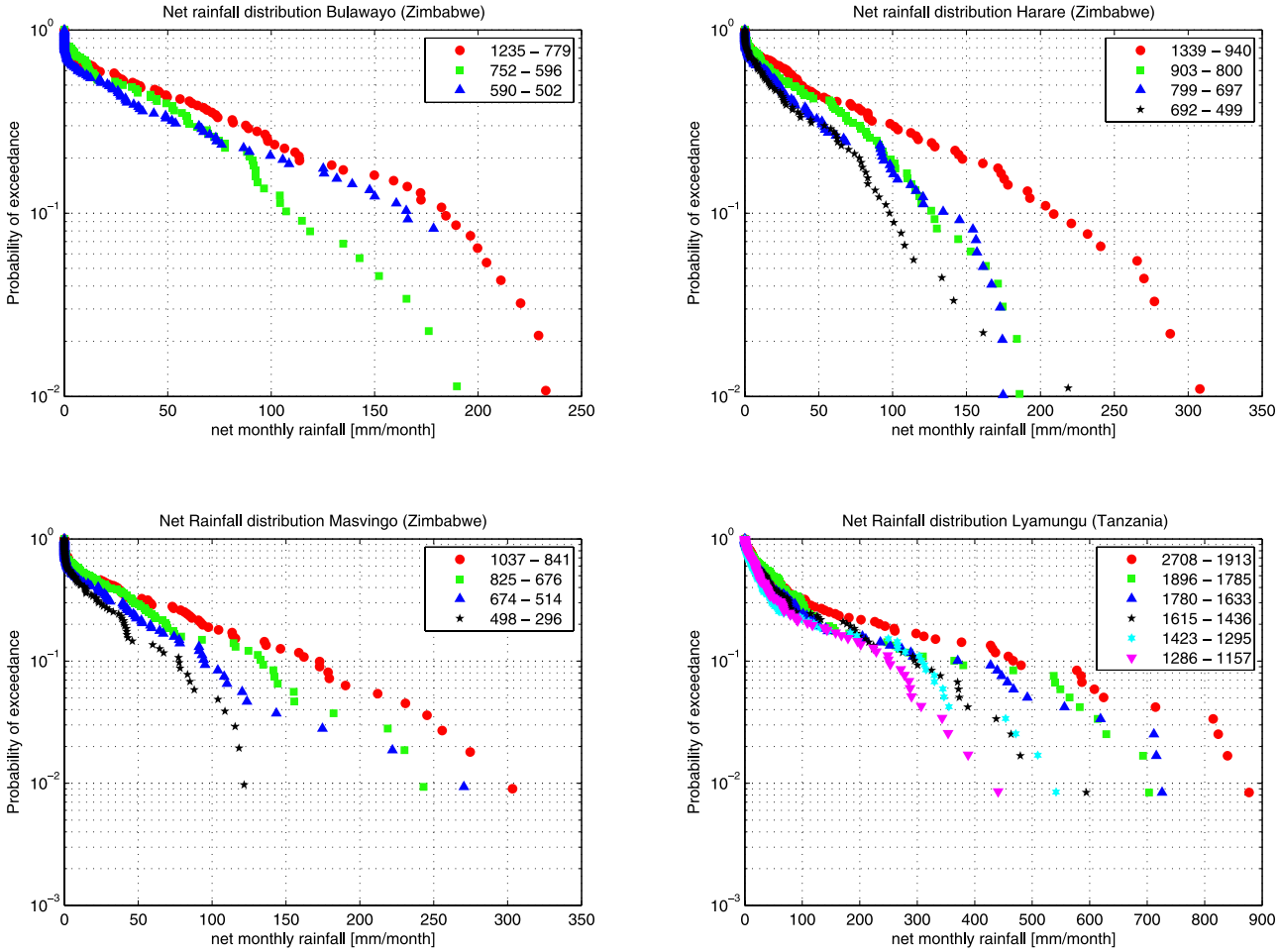

Figure 5. Probability of exceedance of net rainfall amounts on rain months for different stations in Zimbabwe and Tanzania with $D_{i,d}$ = 5 mm/d. The slope equals $-1/\kappa_n$.

[21] The annual interception can be obtained by integration of the product of equations (11) and (13) multiplied with the expected rain months in a year. If we assume $\mathrm{E}(n_{r,d}|n_m)$ to be independent of P_m (which is not true) and assume it as a constant ($\mathrm{E}(n_{r,d}|n_m) \approx n_{r,d}$ = constant), then this can be integrated analytically. In section 4 we shall compute the annual interception numerically without this limiting assumption.

[22] Analytical integration yields [*Oberhettinger and Badii*, 1973, part 1, section 5.34] (see Figure 2c)

$$E_{i,a} = \mathrm{E}(n_{r,m}|n_a)\int_0^\infty E_{i,m}\cdot f_{i,m}(P_m)\mathrm{d}P_m = P_a\left(1 - 2\frac{n_{r,d}D_{i,d}}{\kappa_m}\mathrm{K}_0\left(2\sqrt{\frac{n_{r,d}D_{i,d}}{\kappa_m}}\right)\right) - P_a\left(2\sqrt{\frac{n_{r,d}D_{i,d}}{\kappa_m}}\mathrm{K}_1\left(2\sqrt{\frac{n_{r,d}D_{i,d}}{\kappa_m}}\right)\right) \quad (15)$$

where K_0 and K_1 are Bessel functions of the first and second order, respectively. The fraction $n_{r,d}D_{i,d}/\kappa_m$ is the proportion of the potential amount of annual interception divided by the annual rainfall, which is a sort of aridity index for interception, $\phi_{i,a}$. Equation (15) can then be written as

$$E_{i,a} = P_a\left(1 - 2\phi_{i,a}\mathrm{K}_0\left(2\sqrt{\phi_{i,a}}\right) - 2\sqrt{\phi_{i,a}}\mathrm{K}_1\left(2\sqrt{\phi_{i,a}}\right)\right) \quad (16)$$

3.3. Annual Transpiration Equation (Analytical)

[23] Transpiration is a different process than interception. First, transpiration depends on soil moisture storage and not directly on rainfall. Secondly, the time scale of transpiration is much longer (order of 10 days to several months depending on the soil moisture storage capacity). Often, actual transpiration (E_t) is modeled as potential transpiration ($E_{t,p}$) times a fraction depending on the wetness of the soil [e.g., *Shuttleworth*, 1993]:

$$E_t = E_{t,p}\cdot\min\left(\frac{S}{S_b}, 1\right) \quad (17)$$

where S is the available soil moisture [L] and S_b the available soil moisture below which transpiration is soil moisture contained [L].

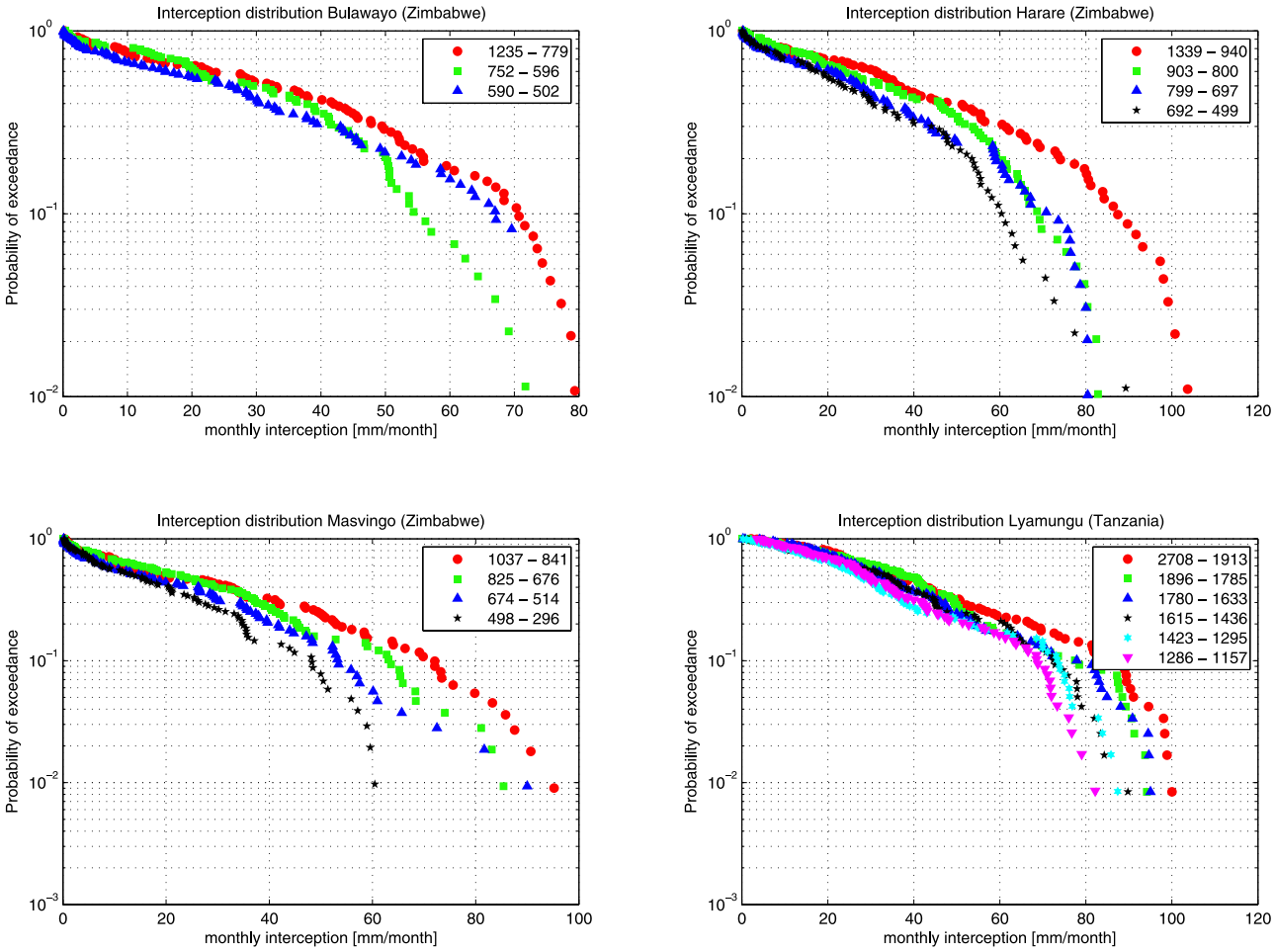

Figure 6. Probability of exceedance of interception amounts for different stations in Zimbabwe and Tanzania with $D_{i,d}$ = 5 mm/day. The slope equals $-1/\kappa_i$.

[24] Although transpiration is not directly dependent on (net) rainfall, *de Groen* [2002] showed that monthly transpiration, $E_{t,m}$ [L T^{-1}], can be described as (see Figure 2d)

$$E_{t,m} = \min\left(A + B \cdot \left(P_m - E_{i,m}\right), D_{t,m}\right) \tag{18}$$

with A the initial soil moisture [L T^{-1}] ("carryover value") and B equal to

$$B = 1 - \gamma + \gamma \exp\left(-\frac{1}{\gamma}\right) \tag{19}$$

where $\gamma = S_b/(D_{t,m} \cdot \Delta t_m)$ and Δt_m equals unity.

[25] While the distribution of monthly rainfall over time can be described with an exponential probability function (equation (13)), we found that this is also valid for the net monthly rainfall. To obtain net monthly rainfall ($P_{n,m}$), monthly interception has been subtracted from the monthly rainfall. Monthly interception is modeled by the expression found by *de Groen and Savenije* [2006] with the implementation of the Markov property of daily rainfall (equation (26)), explained in section 4.1. We could also have used the model presented in section 3.1 (equation (12)); however, *de Groen* [2002] showed that the monthly interception model with Markov properties performed better. Hence we choose the best available monthly interception model. The power functions used for the Markov probabilities are shown in Table 3. In Figure 5 the results are shown. Hence, the distribution function of the net rainfall can be described as

$$f_{t,m}\left(P_{n,m}\right) = \frac{1}{\kappa_n} \exp\left(\frac{-P_{n,m}}{\kappa_n}\right) \tag{20}$$

where κ_n is a function of the monthly interception ($\kappa_n = \kappa_m - \kappa_i$) and κ_i is the scale factor for the monthly interception (see Figure 6).

[26] The average monthly transpiration is then obtained by

$$\begin{aligned}\overline{E}_{t,m} &= \int_0^{D_{t,m}} \left(A + B \cdot P_{n,m}\right) f_{t,m} \mathrm{d}P_{n,m} + \int_{D_{t,m}}^{\infty} D_{t,m} f_{t,m} \mathrm{d}P_{n,m} \\ &= A + \kappa_n B - \kappa_n B \exp\left(\frac{-D_{t,m}}{\kappa_n}\right) \\ &\quad \times \left(\frac{A}{\kappa_n B} + 1 + \frac{D_{t,m}}{\kappa_n} - \frac{D_{t,m}}{\kappa_n B}\right)\end{aligned} \tag{21}$$

[27] When successively multiplied with $\mathrm{E}(n_{nr,m}|n_a) = P_{n,a}/\kappa_n$ and substituting $P_{n,a} = P_a - E_{i,a}$ we obtain the annual transpiration as a function of annual precipitation. Similar to κ_m being linear to P_a, we can assume κ_n to be linear with net monthly rainfall, as can be seen in Figure 7 and Table 3. Of course, this expression is dependent on the daily interception

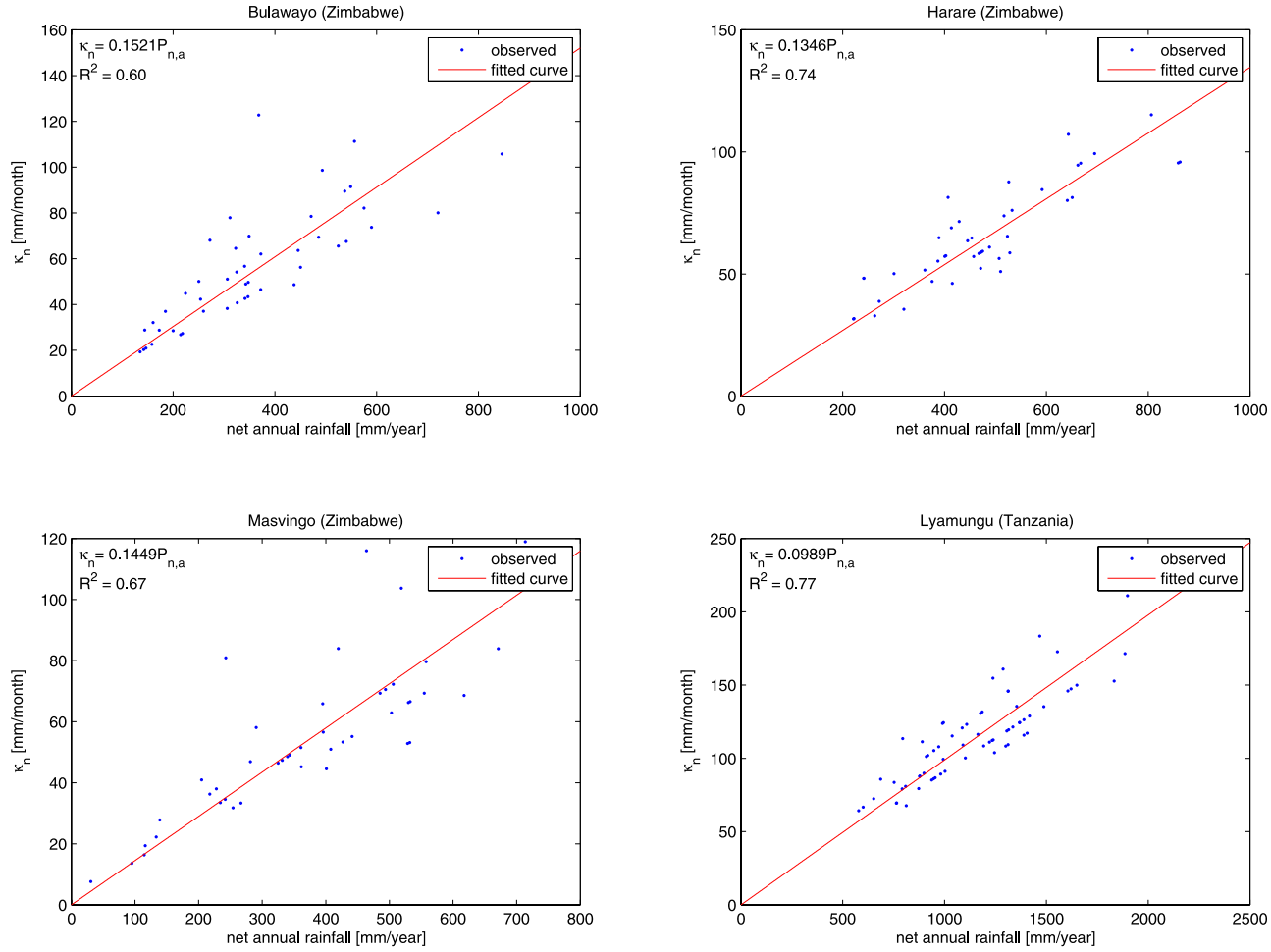

Figure 7. Scaling factor κ_n can be assumed to be directly proportional to the annual rainfall $P_{n,a}$ for given $D_{i,d}$ = 5 mm/d.

threshold, $D_{i,d}$. Hence multiplying equation (21) with $\mathrm{E}(n_{nr,m}|n_a) = P_{n,a}/\kappa_n$ and $P_{n,a} = P_a - E_{i,a}$ results in

$$\begin{aligned} E_{t,a} &= \mathrm{E}(n_{nr,m}|n_a)\cdot\overline{E}_{t,m} = (P_a - E_{i,a})B\left(\frac{A}{\kappa_n B}+1\right) \\ &\quad - (P_a - E_{i,a})B\exp\left(\frac{-D_{t,m}}{\kappa_n}\right)\times\left(\frac{A}{\kappa_n B}+1+\frac{D_{t,m}}{\kappa_n}-\frac{D_{t,m}}{\kappa_n B}\right) \\ &= 2BP_a\left(\phi_{i,a}\mathrm{K}_0\left(2\sqrt{\phi_{i,a}}\right)+\sqrt{\phi_{i,a}}\mathrm{K}_1\left(2\sqrt{\phi_{i,a}}\right)\right) \\ &\quad\times\left(\frac{A}{\kappa_n B}+1-\exp\left(\frac{-D_{t,m}}{\kappa_n}\right)\right. \\ &\quad\left.\times\left(\frac{A}{\kappa_n B}+1+\frac{D_{t,m}}{\kappa_n}-\frac{D_{t,m}}{\kappa_n B}\right)\right) \end{aligned} \tag{22}$$

Introducing $\phi_{t,a} = D_{t,m}/\kappa_n$ as an "aridity" index, this equation becomes (see Figure 2e)

$$\begin{aligned} E_{t,a} &= 2BP_a\left(\phi_{i,a}\mathrm{K}_0\left(2\sqrt{\phi_{i,a}}\right)+\sqrt{\phi_{i,a}}\mathrm{K}_1\left(2\sqrt{\phi_{i,a}}\right)\right) \\ &\quad\times\left(\frac{A}{\kappa_n B}+1-\exp(-\phi_{t,a})\right. \\ &\quad\left.\times\left(\frac{A}{\kappa_n B}+1+\phi_{t,a}-\frac{1}{B}\phi_{t,a}\right)\right) \end{aligned} \tag{23}$$

3.4. Total Evaporation (Analytical)

[28] In the previous subsections annual interception and transpiration have been derived analytically. The total evap-

Table 4. Summary of the Solution of the Analytical Evaporation Model Without Markov Properties[a]

Interception	Transpiration
Daily $E_{i,d} = \min(D_{i,d}, P_d)$	-
Monthly $E_{i,m} = P_m(1 - \exp(-\phi_{i,m}))$	$E_{t,m} = \min(A + B\cdot(P_m - E_{i,m}), D_{t,m})$
Annual $E_{i,a} = P_a(1 - 2\phi_{i,a}\mathrm{K}_0(2\sqrt{\phi_{i,a}}) - 2\sqrt{\phi_{i,a}}\mathrm{K}_1(2\sqrt{\phi_{i,a}}))$	$E_{t,a} = 2BP_a(\phi_{i,a}\mathrm{K}_0(2\sqrt{\phi_{i,a}}) + \sqrt{\phi_{i,a}}\mathrm{K}_1(2\sqrt{\phi_{i,a}}))$ $\times(\frac{A}{\kappa_n B} + 1 - \exp(-\phi_{t,a})(\frac{A}{\kappa_n B} + 1 + \phi_{t,a} - \frac{1}{B}\phi_{t,a}))$

[a]Here $\phi_{i,m} = \frac{D_{i,d}}{\beta}$, $\phi_{i,a} = \frac{n_{r,d}D_{i,d}}{\kappa_m}$ and $\phi_{t,a} = \frac{D_{t,m}}{\kappa_n}$.

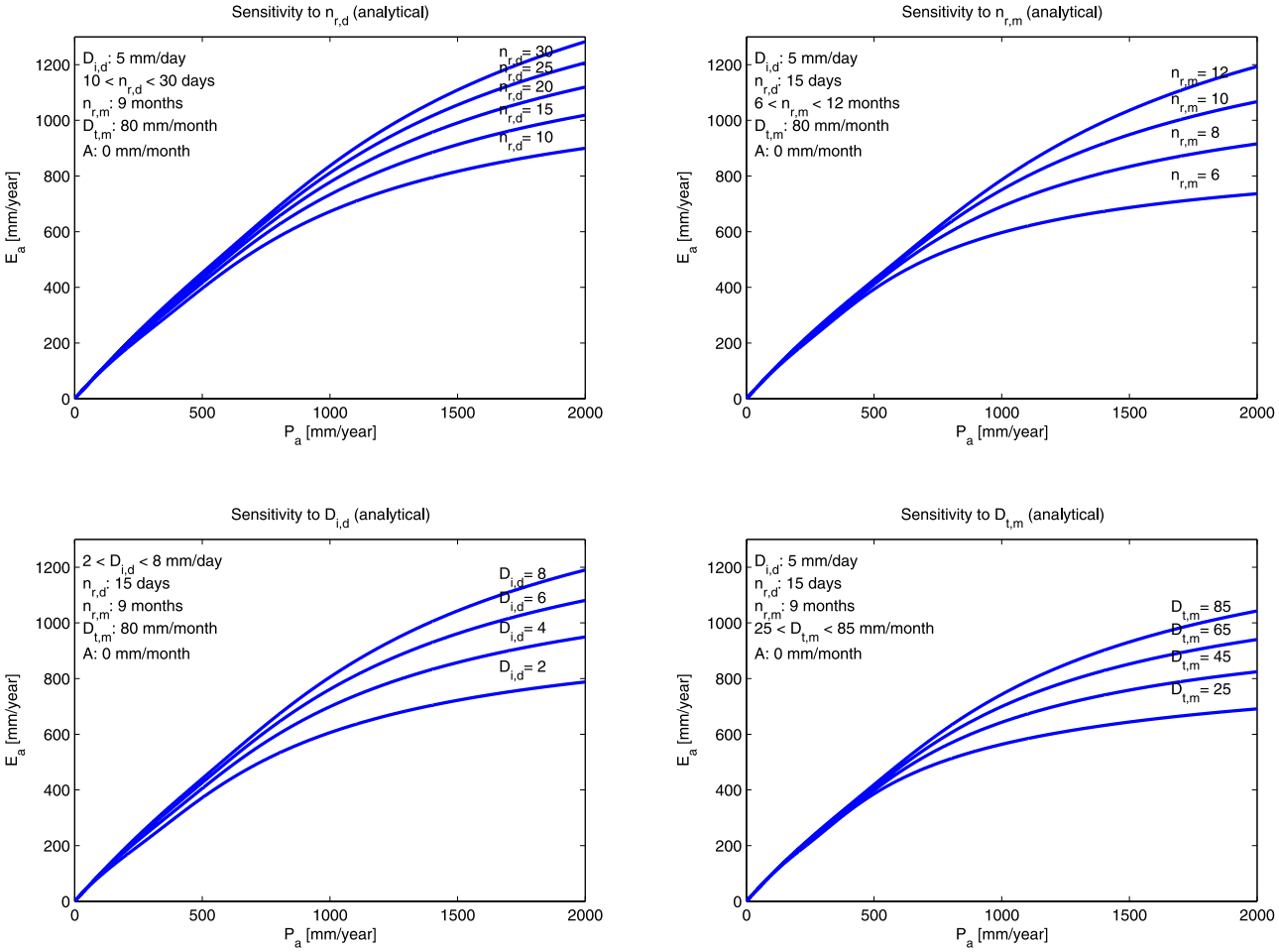

Figure 8. Sensitivity of the parameters of the analytical evaporation model to $n_{r,d}$, $n_{r,m}$, $D_{i,d}$, and $D_{t,m}$ with $\gamma = 0.5$.

oration (E_a) can be obtained by summing up equations (16) and (23). In Table 4 the equations of the analytical solution are summarized.

[29] In Figure 8 the sensitivity of the analytical model to thresholds and rainfall distribution is shown. All model parameters are varied within realistic ranges. The parameter sensitivity is more pronounced for high annual rainfall amounts. From Figure 8 it can be seen that the annual evaporation is obviously sensitive to threshold values, but also to seasonality (the number of rain months ($n_{r,m}$)). An increase of the number of rain months by a factor two, results in an evaporation increase by the same factor two for P_a = 2000 mm/a. Because the uncertainty in the determination of the number of rain months per year (the seasonality) is quite low, this effect is not important at a given location (see also Figure 4).

4. Numerical Derivation With Markov Properties

[30] In the previous section we assumed $E(n_{r,d}|n_m)$ to be constant. However, the expected number of rain days per months is not constant but a function of the monthly rainfall. If the monthly rainfall increases, then the expected number of rain days per month increases as well.

4.1. Monthly Interception Equation (Analytical/Numerical)

[31] *de Groen* [2002] showed that the expected number of rain days per month can be described as

$$\mathrm{E}(n_{r,d}|n_m) = n_m \frac{p_{01}}{1 - p_{11} + p_{01}} \tag{24}$$

By definition p_{11} is the transition probability which gives the probability of a future rain day if the present day is also a rain day. p_{01} is the transition probability, which gives the probability of a future rain day if the present day is a dry day. *de Groen* [2002] showed that these transition probabilities can be described by simple power functions

$$p_{01} = q(P_m)^r \qquad p_{11} = u(P_m)^v \tag{25}$$

With $p_{11} + p_{10} = 1$ and $p_{00} + p_{01} = 1$. The parameters q, r, u and v can be derived from historical daily rainfall data.

[32] In the upscaling equation (11) the expected rain days per months is now considered to depend on P_m, and thus

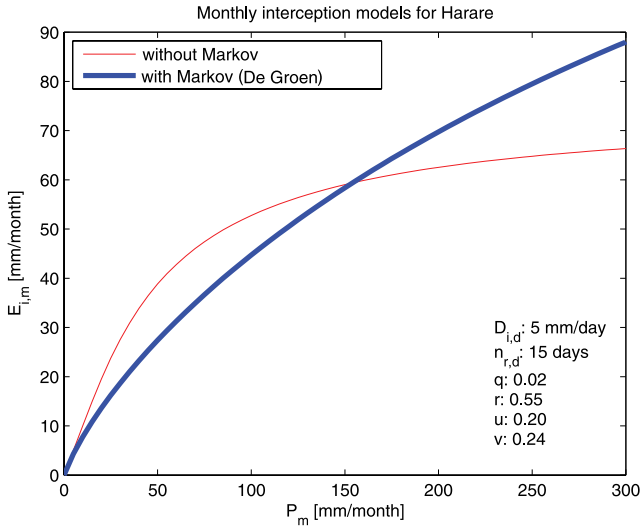

Figure 9. Analytical monthly interception model without Markov properties (equation (12)) and with Markov properties (equation (26)).

$E(n_{r,d}|n_m)$ should be computed with equations (24) and (25). The analytical solution is then [*de Groen and Savenije*, 2006]

$$E_{i,m} = P_m\left(1 - \exp\left(\frac{-D_{i,d}n_m q}{P_m^{1-r} - uP_m^{1-r+v} + qP_m}\right)\right) \quad (26)$$

In Figure 9 this equation is plotted and compared with the analytical solution of equation (12). As can be seen, equation (12) overestimates the low values and underestimates the higher values. This can be explained by the fact that for low rainfall β is higher when the Markov properties are applied. A higher β causes a lower monthly interception and so also a lower annual interception. For high rainfall the opposite is valid.

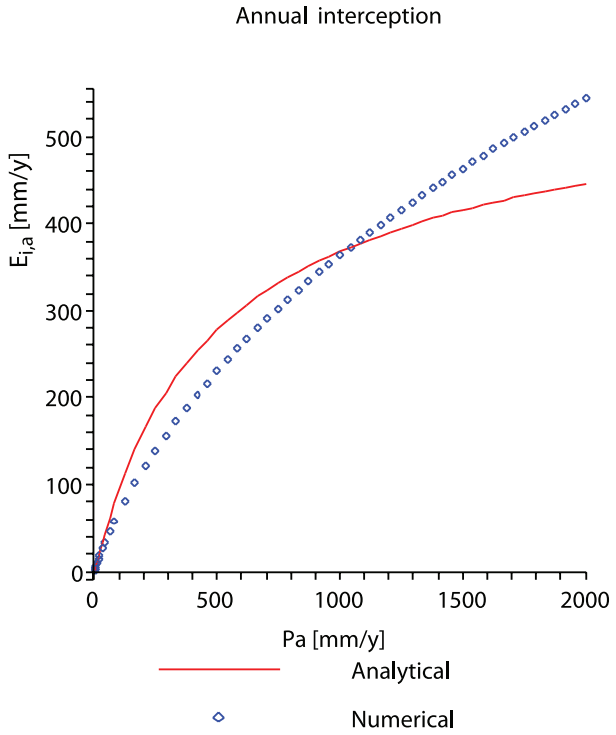

Figure 10. Comparison of the numerical (with Markov properties of Harare) and analytical (without Markov properties, $E(n_{r,d}|n_m)$ = 15 days) annual interception model ($D_{i,d}$ = 5 mm/a and $D_{t,m}$ = 82 mm/month).

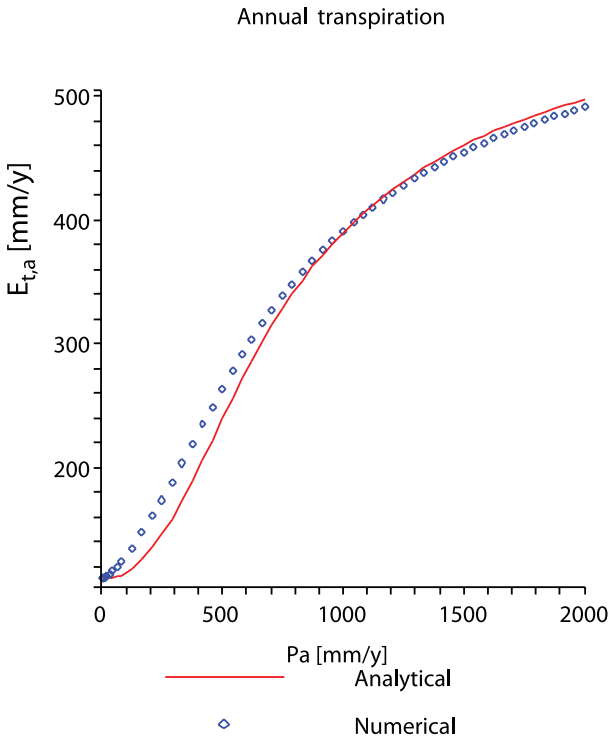

Figure 11. Comparison of the numerical (with Markov properties of Harare) and analytical (without Markov properties, $E(n_{r,d}|n_m)$ = 15 days) annual transpiration model ($D_{i,d}$ = 5 mm/d, $D_{t,m}$ = 82 mm/month, and A = 15 mm/month).

4.2. Annual Interception Equation (Numerical)

[33] In Figure 10 the numerical solution of the annual interception model is shown as circles. As can be seen, the analytical model overestimates interception for low rainfall amounts and underestimates it for high rainfall amounts. This is the result of the deviation in the monthly interception, which is now accumulated.

4.3. Annual Transpiration Equation (Numerical)

[34] The numerical solution for the annual transpiration is shown in Figure 11. In contrast to the interception model, the analytical model underestimates transpiration for low rainfall and overestimates it for high rainfall amounts. This is due to the difference between the analytical and numerical solution of interception. Since $P_{n,a} = P_a - E_{i,a}$ this influences the transpiration results.

4.4. Total Evaporation (Numerical)

[35] The differences between the analytical and numerical interception and transpiration appear to cancel out for the total evaporation at all locations where the rainfall is circa less then about 1500 mm/a. As an illustration the results for Harare are shown in Figure 12. From this graph we can see that the difference between the analytical and the numerical model are small as long as the annual rainfall is less than 1500 mm/a.

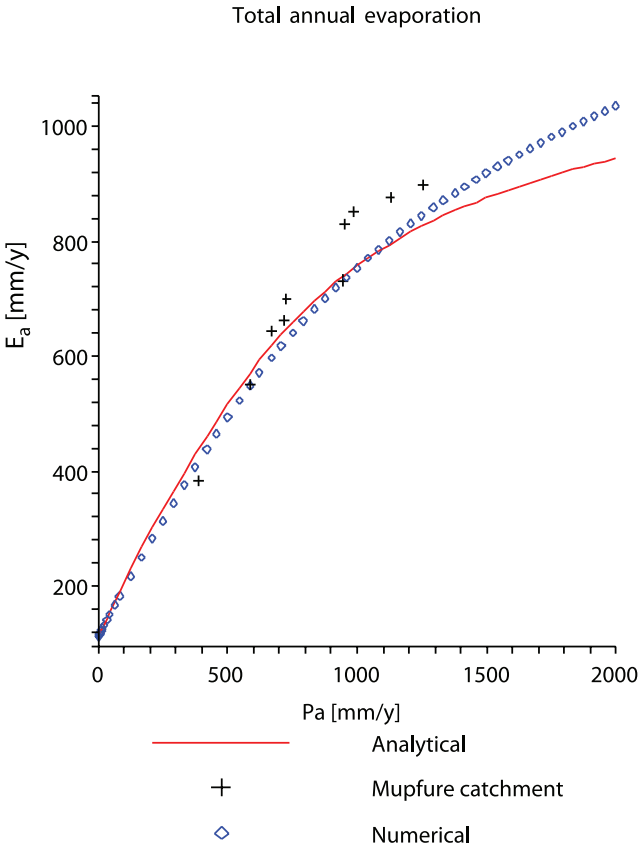

Figure 12. Comparison of the numerical (with Markov properties of Harare) and analytical (without Markov properties, $E(n_{r,d}|n_m) = 15$ days) annual evaporation model ($D_{i,d} = 5$ mm/d, $D_{t,m} = 82$ mm/month, and $A = 15$ mm/month) and observed data from the Mupfure catchment (Zimbabwe).

[36] The crosses in Figure 12 show observations of the Mupfure catchment at Beatrice in Zimbabwe from 1970 to 1979 [*Savenije*, 2004]. The Mupfure River lies southwest of Harare. At Beatrice the basin has an area of circa 1215 Mm^2. Although Harare is located just outside the Mupfure catchment (circa 50 km northwest of Beatrice), the observations at Beatrice are assumed to be highly correlated with our findings for Harare. It appears that our formula underestimates the annual total evaporation. The most likely cause of this discrepancy is that in the Mupfure catchment intensive irrigation takes place, which causes higher actual evaporation than in an undisturbed catchment where evaporation is calculated as the difference between precipitation and runoff [*Mazvimavi*, 1998]. IWRMS (The Mupfure catchment, 2001, available at http://www.geogr.uni-jena.de//fileadmin/Geoinformatik/projekte/iwrms/) estimated that this water use amounts to about 40 mm/a. Another reason for the discrepancy is that in the Mupfure basin the number of rain days is slightly higher than in Harare.

5. From Evaporation Model to Budyko Curve

[37] In Figure 13 the results of our model are compared with the different types of Budyko curves. In our approach each location appears as a single dot for every year. In principle at a given location a dot can be produced if P_a, E_p and rainfall characteristics are known. Here we only had one long-term average value for E_p which was combined with the average annual rainfall characteristics. The number of rain days (i.e., days with more rainfall than 0.1 mm/day) are obtained from the CRU TS 2.1 data set [*Mitchell and Jones*, 2005]. Furthermore, for all locations a daily interception threshold ($D_{i,d}$) of 5 mm/day has been used. The monthly transpiration threshold, $D_{t,m}$ is calculated as $(E_p - E_{i,a})/n_a$, which means that the interception process is considered to absorb the available energy first, while only the remaining potential evaporation is available for transpiration.

6. Discussion

[38] The results presented in Figure 13 deviate from the classical Budyko curves. For some locations our results yield more evaporation than predicted by the existing curves while others yield less. In general, locations with a distinct monsoon season, like southern Africa, underestimate evaporation and, are closer to *Schreiber*'s [1904] curve, while others are closer to *Budyko*'s [1974] curve. In order to explain this discrepancy, we looked at the possible effect of the most sensitive parameter: $n_{r,m}$, the number of rain months per year. This is the indicator for a climate with a distinct dry and wet season (see Figure 8). In Figure 13 the range of possible outcomes is presented. The upper bound corresponds with 12 rain months per year and the lower bound represents 6 rain months per year. It is clear that the monsoon effect cannot explain the discrepancy. However, it is clear that the outliers are from stations with a clear dry season.

[39] Another possible explanation was mentioned by *Budyko* [1974] and *Potter et al.* [2005]. They found systematic deviations for certain catchments and they explained the effect by seasonality. They observed that locations where monthly potential evaporation and precipitation rates are in phase, in general are overestimated the classical Budyko curves. Locations where the potential evaporation and precipitation are out of phase, are generally underestimated. *Milly* [1994] investigated this process in more detail. He developed a model where he incorporated seasonality and demonstrated that he could explain the deviations. In our locations we see the same: the locations that are out of phase plot below the curves, and those that are in phase plot higher.

[40] A possible reason for this effect could be vegetation as also suggested by *Milly and Dunne* [1994]. In areas where potential evaporation and precipitation are out of phase, for example in semiarid regions, vegetation has been adapted to the rainfall pattern. In times of droughts, plants can withdraw water from deeper layers by developing a deep root system. Hence they still can transpire even during the dry season. This process can be modeled by the carryover factor A of equation (23). If we estimate a reasonable value for this water consumption from deeper layers (see Table 3), our results improve significantly. In Figure 14 the results are shown. These results should be seen as an indication of the amount of the annual carry over required to compensate for seasonality, and not as a confirmation of this process. Further research is required to test this hypothesis.

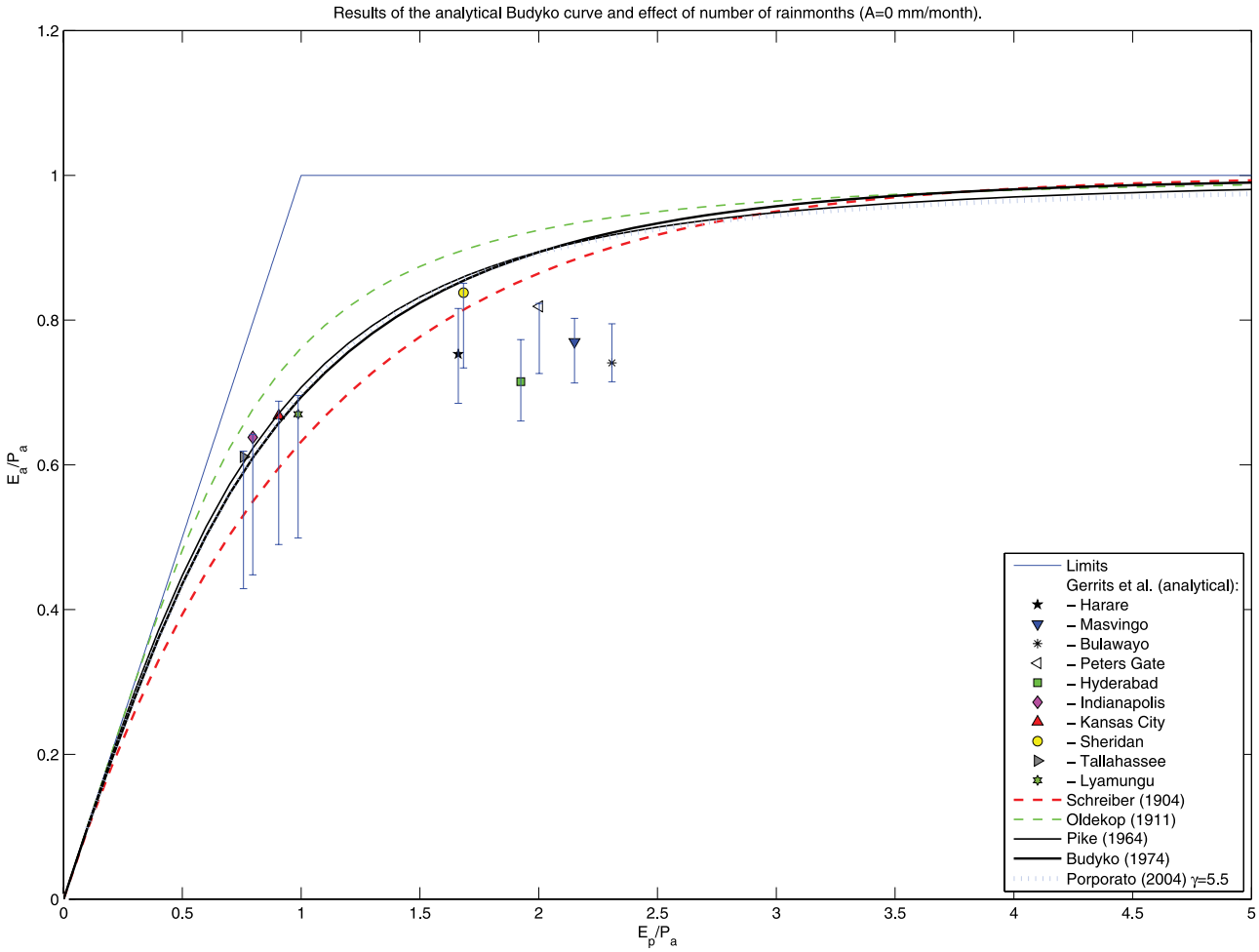

Figure 13. Results of the analytical model for the ten locations and the different classical Budyko curves as well as the effect of number of rain months on the Budyko curve. The lower bound represents a number of rain months of 6 and the upper bound a number of rain months of 12.

[41] Another seasonality effect is the change in interception threshold, $D_{i,d}$ and transpiration threshold, $D_{t,m}$ throughout the seasons. In our approach, we use a constant value. By neglecting the seasonality of the transpiration threshold an error is made, since most vegetation has a distinct growing and dormant period. However, one may question if this is a wrong assumption for the interception process. Often it is concluded that the interception capacity changes throughout the year [e.g., *Link et al.*, 2004; *Loustau et al.*, 1992]. During summer time higher canopy storage capacity values are observed, because deciduous trees still have leaves. During fall, the trees drop their leaves, so the canopy storage capacity is less. However, in our model interception is not only defined as canopy interception, but as the sum of canopy and forest floor interception. When a tree loses its leaves, they fall on the ground and stay there for a long time. Hence, one might expect that the total interception capacity remains the same (or does not differ much) over the year.

7. Conclusions

[42] A lot of research has been done on finding the relation between the aridity index and actual evaporation as a function of annual precipitation. Although observations do not fully agree with empirical relationships, all these curves have similar shapes. The model presented in this paper lies within the range of these curves and the scatterplots generated by observations. The evaporation model distinguishes between interception and transpiration. Interception is modeled as a threshold process on daily time scale. It is upscaled by equation (11) making use of the daily rainfall characteristics and the expected rain days per month. Successively, monthly interception is upscaled to annual interception, making use of the rainfall distribution of monthly rainfall. Also transpiration can be modeled as a threshold process on a monthly time scale and successively upscaled to annual transpiration. For the expected rain days per month two equations are used. One where the number of rain days is considered linear to the monthly rainfall and one where the Markov probabilities of daily rainfall are used. The first equation can be solved analytically and is summarized in Table 4. The equation with Markov properties could not be solved analytically, hence it is solved numerically.

[43] The analytical and numerical solutions differ for interception and transpiration, but when added up, the difference in the total evaporation is less. If the model output is compared with measured data from Harare, we can

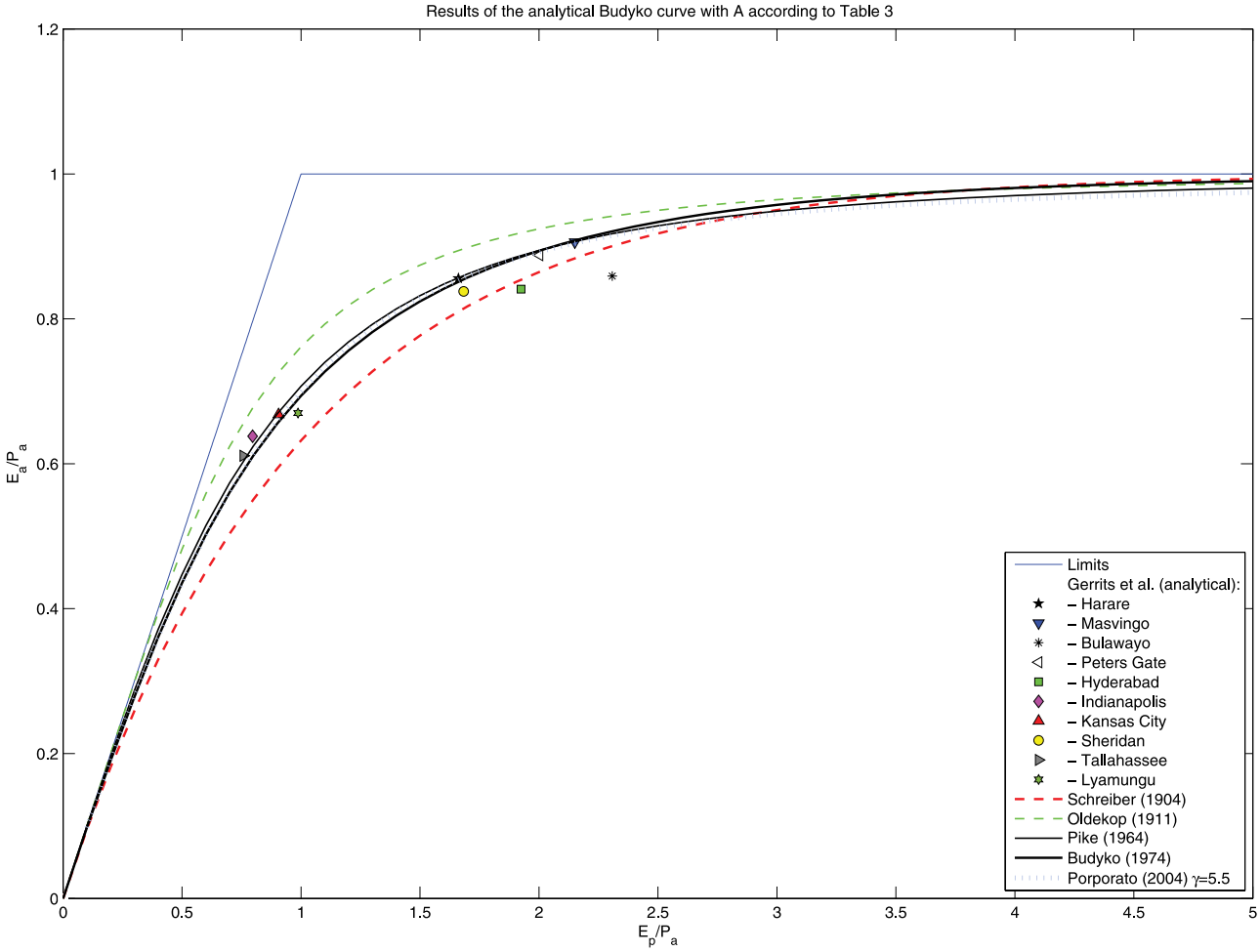

Figure 14. Results of the analytical model for the ten locations and the different classical Budyko curves when taking deep root systems into account.

conclude that the annual evaporation model preforms quite well for this location.

[44] Since the analytical and the numerical solutions do not differ much, we applied the analytical model for ten locations around the world in different climates. The results look promising and do not deviate much from the classical Budyko curves. Remarkable is the fact that locations with a distinct rainy season are below the existing curves and the others are on the formula found by *Budyko* [1974], yielding highest evaporation to precipitation ratios. *Budyko* [1974], *Potter et al.* [2005], and *Milly* [1994] gave a possible explanation for this. They claim that this can be caused by the phase difference between potential evaporation and rainfall. When a carryover factor, A, is used for semiarid areas (which takes into account that plants can withdraw water from deeper layers by developing a deep root system) the results improve significantly.

[45] Concluding, the analytical model, with only five (measurable) parameters, is capable of representing the Budyko curve. However, further research is necessary on the seasonality of the thresholds for interception and transpiration.

Notation

E_i evaporation from interception [L T^{-1}].
E_t transpiration [L T^{-1}].
E actual evaporation [L T^{-1}].
E_o open water evaporation [L T^{-1}].
E_s soil evaporation [L T^{-1}].
E_p potential evaporation [L T^{-1}].
$D_{i,d}$ interception threshold (daily) [L T^{-1}].
$D_{t,m}$ transpiration threshold (monthly) [L T^{-1}].
β scaling factor for daily rainfall [L T^{-1}].
$\kappa_{i,m,n}$ scaling factor for monthly interception, rainfall and net rainfall, respectively [L T^{-1}].
ϕ aridity index [−].
λ latent heat of vaporization coefficient [L^2 T^{-2}].
ρ density of water [M L^{-3}].
γ time scale for transpiration (= $S_b/D_{t,m}$)[T].
$n_{r,d}$ number of rain days per month [−].
$n_{r,m}$ number of rain months per year [−].
$n_{nr,m}$ number of net rain months per year [−].
n_m days within a month (= 30.5) [−].
n_a months within a year (= 12) [−].
p_{01} Markov probability of rain day 1 occurring after dry day 0 [−].
q constant in $p_{01} = q(P_m)^r$ [(T L^{-1})^r].
r power in $p_{01} = q(P_m)^r$ [−].
u constant in $p_{11} = u(P_m)^v$ [(T L^{-1})^v].
v power in $p_{11} = u(P_m)^v$ [−].
P precipitation [L T^{-1}].
P_n net precipitation [L T^{-1}].

S_b available soil moisture content at the boundary between moisture constrained transpiration and potential transpiration [L].
S water storage [L].
Q runoff [L T^{-1}].
R_n net radiation [M T^{-3}].
H sensible heat flux [M T^{-3}].
G ground heat flux [M T^{-3}].
B_r Bowen ratio [−].
A monthly moisture carry over for transpiration [L T^{-1}].
B slope of relation between monthly effective rainfall and monthly transpiration [−].

[46] **Acknowledgments.** The authors would like to thank the Ministry of Culture, Higher Education and Research of Luxembourg and Delft Cluster, the Netherlands, for their support of this research. Furthermore, we would like to thank Benjamin Fischer and Hessel Winsemius for their data.

References

Arora, V. K. (2002), The use of the aridity index to assess climate change effect on annual runoff, *J. Hydrol.*, *265*, 164–177.

Baird, A. J., and R. L. Wilby (1999), *Eco-hydrology: Plants and Water in Terrestrial and Aquatic Environments*, Routledge, London.

Budyko, M. I. (1974), *Climate and Life*, Academic, Orlando, Fla.

Choudhury, B. J. (1999), Evaluation of an empirical equation for annual evaporation using field observations and results from a biophysical model, *J. Hydrol.*, *216*, 99–110.

de Groen, M. M. (2002), *Modelling Interception and Transpiration at Monthly Time Steps: Introducing Daily Variability Through Markov Chains*, Swets and Zeitlinger, Lisse, Netherlands.

de Groen, M. M., and H. H. G. Savenije (2006), A monthly interception equation based on the statistical characteristics of daily rainfall, *Water Resour. Res.*, *42*, W12417, doi:10.1029/2006WR005013.

Deguchi, A., S. Hattori, and H. Park (2006), The influence of seasonal changes in canopy structure on interception loss: Application of the revised Gash model, *J. Hydrol.*, *318*, 80–102.

Dolman, A. J., and D. Gregory (1992), The parametrization of rainfall interception in GCMS, *Q. J. R. Meteorol. Soc.*, *118*(505), 455–467.

Donohue, R. J., M. L. Roderick, and T. R. McVicar (2007), On the importance of including vegetation dynamics in Budyko's hydrological model, *Hydrol. Earth Syst. Sci.*, *11*, 983–995.

Gerrits, A. M. J., H. H. G. Savenije, L. Hoffmann, and L. Pfister (2007), New technique to measure forest floor interception - an application in a beech forest in Luxembourg, *Hydrol. Earth Syst. Sci.*, *11*, 695–701.

Gerrits, A. M. J., H. H. G. Savenije, and L. Pfister (2009), *Canopy and Forest Floor Interception and Transpiration Measurements in a Mountainous Beech Forest in Luxembourg*, *IAHS Redbook*, Int. Assoc. of Hydrol. Sci., in press.

Helvey, J. D., and J. H. Patric (1965), Canopy and litter interception of rainfall by hardwoods of eastern United States, *Water Resour. Res.*, *1*(2), 193–206.

Link, T. E., M. Unsworth, and D. Marks (2004), The dynamics of rainfall interception by a seasonal temperate rainforest, *Agric. For. Meteorol.*, *124*(3–4), 171–191.

Loustau, D., P. Berbigier, and A. Granier (1992), Interception loss, throughfall and stemflow in a maritime pine stand. II. An application of Gash's analytical model of interception, *J. Hydrol.*, *138*, 469–485.

Mazvimavi, D. (1998), Water resources management in the water catchment board pilot areas, phase 1: Data collection, technical report, Cent. for Appl. Social Sci., Univ. of Zimbabwe, Harare.

Milly, P. C. D. (1993), An analytic solution of the stochastic storage problem applicable to soil water, *Water Resour. Res.*, *29*(11), 3755–3758.

Milly, P. C. D. (1994), Climate, soil water storage, and the average annual water balance, *Water Resour. Res.*, *30*(7), 2143–2156.

Milly, P. C. D., and K. A. Dunne (1994), Sensitivity of the global water cycle to the water-holding capacity of land, *J. Clim.*, *7*, 506–526.

Mitchell, T. D., and P. D. Jones (2005), An improved method of constructing a database of monthly climate observations and associated high-resolution grids, *Int. J. Climatol.*, *25*(6), 693–712.

Oberhettinger, F., and L. Badii (1973), *Tables of Laplace Transformations*, Springer, Berlin.

Ol'dekop, E. M. (1911), On evaporation from the surface of river basins, *Trans. Meteorol. Obs.*, *4*, 200.

Perrin, C., L. Oudin, V. Andreassian, C. Rojas-Serna, C. Michel, and T. Mathevet (2007), Impact of limited streamflow data on the efficiency and the parameters of rainfall-runoff models, *Hydrol. Sci. J.*, *52*, 131–151.

Pike, J. G. (1964), The estimation of annual runoff from meteorological data in a tropical climate, *J. Hydrol.*, *2*, 116–123.

Porporato, A., E. Daly, and I. Rodriguez-Iturbe (2004), Soil water balance and ecosystem response to climate change, *Am. Nat.*, *164*(5), 625–632.

Potter, N. J., L. Zhang, P. C. D. Milly, T. A. McMahon, and A. J. Jakeman (2005), Effects of rainfall seasonality and soil moisture capacity on mean annual water balance for Australian catchments, *Water Resour. Res.*, *41*, W06007, doi:10.1029/2004WR003697.

Priestley, C. H. B., and R. J. Taylor (1972), On the assessment of surface heat flux and evaporation using large-scale parameters, *Mon. Weather Rev.*, *100*, 81–91.

Rodríguez-Iturbe, I., and A. Porporato (2004), *Ecohydrology of Water-Controlled Ecosystems*, Cambridge Univ. Press, Cambridge, U. K.

Rutter, A. J., K. A. Kershaw, P. C. Robins, and A. J. Morton (1971), A predictive model of rainfall interception in forests. I. Derivation of the model and comparison with observations in a plantation of Corsican pine, *Agric. Meteorol.*, *9*, 367–384.

Samuel, J. M., M. Sivapalan, and I. Struthers (2008), Diagnostic analysis of water balance variability: A comparative modeling study of catchments in Perth, Newcastle, and Darwin, Australia, *Water Resour. Res.*, *44*, W06403, doi:10.1029/2007WR006694.

Savenije, H. H. G. (1997), Determination of evaporation from a catchment water balance at a monthly time scale, *Hydrol. Earth Syst. Sci.*, *1*, 93–100.

Savenije, H. H. G. (2004), The importance of interception and why we should delete the term evapotranspiration from our vocabulary, *Hydrol. Processes*, *18*, 1507–1511.

Schreiber, P. (1904), Über die Beziehungen zwischen dem Niederschlag und der Wasserführung der Flüsse in Mitteleuropa, *Z. Meteorol.*, *21*(10), 441–452.

Scott, R., R. D. Koster, D. Entekhabi, and M. J. Suarez (1995), Effect of a canopy interception reservoir on hydrological persistence in a general circulation model, *J. Clim.*, *8*, 1917–1921.

Shuttleworth, W. J. (1993), *Handbook of Hydrology*, chap. 4, pp. 4.1–4.53, McGraw-Hill, New York.

Sivapalan, M., and G. Blöschl (1998), Transformation of point rainfall to areal rainfall: Intensity-duration-frequency curves, *J. Hydrol.*, *204*, 150–167.

Todorovic, P., and D. A. Woolhiser (1975), A stochastic model of *n*-day precipitation, *J. Appl. Meteorol.*, *14*, 17–24.

Turc, L. (1954), Le bilan d'eau des sols. Relation entre la précipitation, l'évaporation et l'écoulement, *Ann. Agron.*, *5*, 491–569.

Viville, D., P. Biron, A. Granier, E. Dambrine, and A. Probst (1993), Interception in a mountainous declining spruce stand in the Strengbach catchment (Vosges, France), *J. Hydrol.*, *144*, 273–282.

Woolhiser, D. A., T. O. Keefer, and K. T. Redmond (1993), Southern oscillation effects on daily precipitation in the southwestern United States, *Water Resour. Res.*, *29*(4), 1287–1295.

Yang, D., F. Sun, Z. Liu, Z. Cong, and Z. Lei (2006), Interpreting the complementary relationship in non-humid environments based on the Budyko and Penman hypotheses, *Geophys. Res. Lett.*, *33*, L18402, doi:10.1029/2006GL027657.

Yang, H., D. Yang, Z. Lei, and F. Sun (2008), New analytical derivation of the mean annual water-energy balance equation, *Water Resour. Res.*, *44*, W03410, doi:10.1029/2007WR006135.

Zhang, L., W. R. Dawes, and G. R. Walker (2001), Response of mean annual evapotranspiration to vegetation changes at catchment scale, *Water Resour. Res.*, *37*(3), 701–708.

Zhang, L., K. Hickel, W. R. Dawes, F. H. S. Chiew, A. W. Western, and P. R. Briggs (2004), A rational function approach for estimating mean annual evapotranspiration, *Water Resour. Res.*, *40*, W02502, doi:10.1029/2003WR002710.

A. M. J. Gerrits, H. H. G. Savenije, and E. J. M. Veling, Water Resources Section, Delft University of Technology, Stevinweg 1, NL-2628 CN Delft, Netherlands. (a.m.j.gerrits@tudelft.nl)

L. Pfister, Department of Environment and Agro-biotechnologies, Centre de Recherche Public-Gabriel Lippmann, 41 rue du Brill, L-4422 Belvaux, Luxembourg.